Title	Very large phase shift of microwave signals in a 6 nm Hf x Zr 1– x O 2 ferroelectric at ±3 V
Authors	Dragoman, Mircea;Modreanu, Mircea;Povey, Ian M.;Iordanescu, Sergiu;Aldrigo, Martino;Romanitan, Cosmin;Vasilache, Dan;Dinescu, Adrian;Dragoman, Daniela
Publication date	2017-08-31
Original Citation	Dragoman, M., Modreanu, M., Povey, I. M., Iordanescu, S., Aldrigo, M., Romanitan, C., Vasilache, D., Dinescu, A. and Dragoman, D. (2017) 'Very large phase shift of microwave signals in a 6 nm Hf x Zr 1– x O 2 ferroelectric at ±3 V', Nanotechnology, 28(38), 38LT04 (5pp). doi:10.1088/1361-6528/aa8425
Type of publication	Article (peer-reviewed)
Link to publisher's version	10.1088/1361-6528/aa8425
Rights	© 2017 IOP Publishing Ltd. This is an author-created, un-copyedited version of an article accepted for publication in Nanotechnology. The publisher is not responsible for any errors or omissions in this version of the manuscript or any version derived from it. The Version of Record is available online at https://doi.org/10.1088/1361-6528/aa8425
Download date	2024-05-13 06:50:40
Item downloaded from	https://hdl.handle.net/10468/4640

Very large phase shift of microwave signals in a 6nm $Hf_xZ_{1-x}rO_2$ ferroelectric at ±3V

Mircea Dragoman[1*], Mircea Modreanu[2], Ian M. Povey[2], Sergiu Iordanescu[1], Martino Aldrigo[1],

Cosmin Romanitan[1,3], Dan Vasilache[1], Adrian Dinescu[1], Daniela Dragoman[3,4]

[1]National Institute for Research and Development in Microtechnology (IMT), P.O. Box 38-160,

023573 Bucharest, Romania,

[2]Tyndall National Institute, Lee Maltings Complex, Dyke Parade, Cork, Ireland

[3]Univ. Bucharest, Physics Faculty, P.O. Box MG-11, 077125 Bucharest, Romania

[4]Academy of Romanian Scientists, Splaiul Independentei 54, 050094 Bucharest, Romania

Abstract In this letter, we report for the first time very large phase shifts of microwaves in the 1-10 GHz range, in a 1-mm-long gold coplanar interdigitated structure deposited over 6 nm $Hf_xZr_{1-x}O_2$ ferroelectric grown directly on a high-resistivity silicon substrate. The phase shift is larger than 60° at 1 GHz and 13° at 10 GHz at maximum applied DC voltages of ± 3 V, which can be supplied by a simple commercial battery. In this way, we demonstrate experimentally that the new ferroelectrics based on HfO_2 could play an important role in the future development of wireless communication systems for very low power applications.

*Corresponding author. Email: mircea.dragoman@imt.ro

2

1. Introduction

The ferroelectric behavior of HfO_2 was discovered few years ago, by slightly doping HfO_2 – a widespread gate insulator in transistors and very large scale integrated circuits such as microprocessors, which can be retrieved in any laptop or desktop computers and mobile phones. The ferroelectric HfO_2 is only few nm thick, the ferroelectric phase being attributed to an orthorhombic crystalline structure. The physical mechanisms producing the ferroelectric phase in HfO_2 doped with various dopants, in particular Zr used in this paper, are well described in Refs. [1-2] by the group of authors who discovered the ferroelectricity in HfO_2, and in the comprehensive review in Ref. [3]. $Hf_xZr_{1-x}O_2$ ferroelectrics are now the subject of intense researches about their piezoelectric properties [4], pyroelectric response [5] and tunneling electroresistance [6].

In a very recent paper, we have shown that ferroelectrics based on doped HfO_2 confer extraordinary tunability to microwave circuits [7], which is a precondition for developing wireless communication circuits and systems that must satisfy simultaneously the following properties: (i) be miniaturized, (b) be tunable, i.e. have the ability to work at various electromagnetic bandwidths on demand, and (c) have low energy consumption. These prerequisites are difficult to be satisfied by perovskite ferroelectrics, used in the past as tunable microwave materials, because they are not fully CMOS compatible and their energy consumption is high; for example, tens of volts are necessary to obtain a significant phase shift in the microwave domain using perovskite ferroelectrics. On the contrary, HfO_2-based ferroelectrics are fully CMOS compatible and can be scaled down up to a thickness of 2-3 nm, i.e. up to becoming an atomically thick material, such that a significant tunability of various circuits, in particular filters or phase shifters, is achieved at few volts.

Phase shifters of electromagnetic waves are especially used as phased antenna arrays (PAAs). However, the utilization of perovskite ferroelectrics as phase shifters in PAAs is almost abandoned today, because they require high DC voltages, exceeding tens of volts, and rather

high losses [8]. The PAAs have many applications in daily life, and huge applications in communications and applied physics. Weather and airplane radars, space communications, as well as smart phones and base stations for 4G and 5G wireless communications are widespread applications of PAAs. Astrophysics and radio-telescopes are other beneficiaries of the phased arrays [9]. Therefore, it is of outmost importance to develop phase shifters that can be easily integrated in PAAs. In addition, these phase shifters must be able to satisfy the increasing demand of PAAs, which are among the few systems able to emit/receive electromagnetic waves in a crowded spectrum shared by billions of users. The aim of this paper is to demonstrate that a $Hf_xZr_{1-x}O_2$ ferroelectric phase shifter is able to produce significant phase shifts at low applied voltages, becoming thus an interesting choice for future PAAs.

2. Fabrication and structural characterization

The scanning electron microscope (SEM) image of a phase shifter based on a $Hf_xZr_{1-x}O_2$ ferroelectric and the optical microscope image are represented in Fig. 1(a). The coplanar structure consists of three Au electrodes, with a thickness of 200 nm deposited over 6 nm $Hf_xZr_{1-x}O_2$, grown on a 500 µm-thick high resistivity Si substrate. The central (signal) electrode of the CPW has a width of 100 µm, and it is separated from the outer ground electrodes by a gap of 50 µm. The length of the interdigitated capacitor (IDC) embedded in the central conductor is 200 µm and each digit has a width of 5 µm, two consecutive digits being distanced by 10 µm. The transition between the IDC and the CPW electrodes is achieved by a taper.

The nominally 6-nm-thick $Hf_xZr_{1-x}O_2$ films were grown at $250^{o}C$ on high resistivity Si (100) substrates by Atomic Layer Deposition (ALD) using a Cambridge NanoTech F200 ALD reactor. The ALD precursors were Tetrakis(ethylmethylamido)hafnium (TEMAHf), Tetrakis (ethylmethylamido)zirconium (TEMAZr) and water. Growth was performed in a laminate ALD mode using 30 super-cycles of TEMAZr-H_2O-TEMAHf-$H_2$0, all separated by argon purges. The film thickness was confirmed by spectroscopic ellipsometry (Woollam M2000) to be 5.6±0.2 nm using a four layer optical model: air/$Hf_xZr_{1-x}O_2$/SiO_2/Si [1]. The composition of the nominally

4

$Hf_xZr_{1-x}O_2$ films was investigated by X-ray photoelectron spectroscopy (XPS) using a Kratos AXIS ULTRA spectrometer with a source of monochromatic Al K_α of 1486.58 eV. The nominally $HfZrO_4$ films are clearly non stoichiometric ($Hf_{0.45}Zr_{0.55}O_{1.76}$), due to a small differences in the metal growth rates, and a significant oxygen deficiency (see Table I). Furthermore, the XPS data implies that this oxygen deficiency can be more likely attributed to ZrOx species. The grazing incidence X-ray diffraction (GIXRD) pattern of the $Hf_{0.45}Zr_{0.55}O_{1.76}$ film has have been measured on a Rigaku Smartlab system using the Cu K_α line at an angle of incidence of 0.35^o. The GIXRD pattern is presented in Fig. 1(b), and shows two broad peaks, at around 30.5^o and 55°, which were previously assigned to $(111)_O$ and $(022)_O/(220)_O$ reflections for the HfO_2 orthorhombic phase with Pbc21 symmetry [1, 10, 11]. The Cr (5nm)/Au (200nm) electrodes were finally deposited using a Temescal FC200 e-beam evaporation system and have been photolithographic configured using a standard lift-off process.

3. Measurements and discussions

The ferroelectric phase shifters are measured directly on-wafer with a vector network analyzer (VNA)-Anritsu-37397D connected to a Karl-Suss PM5 on-wafer probe station. The SOLT calibration standard was used to calibrate the system before measurements of the devices. During measurements, the calibration was verified few times to see if the accuracy is preserved. The set-up is schematically represented in Fig. 2. The ferroelectric phase shifters were biased by an external DC source, which is able to control very precisely the supplied DC voltage. The bias is applied vertically on the entire structure, conferring to the $Hf_{0.45}Zr_{0.55}O_{1.76}$ ferroelectric a DC polarization via a vertical electric field.

The phase shift of microwave signals in the range of 1-10 GHz at various voltages, in the range ± 3 V, is represented in Fig. 3(a) at room temperature. The phase shift is defined as $\Delta\varphi = \varphi_{V_{DC}} - \varphi_{0V}$, i.e. as the difference between the phases acquired at a certain DC voltage and at 0 V. At a certain frequency, the modulus of the phase shift increases as the voltage increases.

However, at biases higher than +3 V no significant increase in the phase shift is observed due to saturation of the ferroelectric response.

Hundreds of phase shifters were fabricated on the same wafer, all of them showing almost identical characteristics. Moreover, the measurements were repeated on a daily basis for more than one month on 10 devices located arbitrarily on the wafer, in order to verify the reproducibility of the results in Fig. 3(a). No significant changes were observed during this period.

The total phase shift of the device when polarized at +3 V and -3 V, defined as $\Delta\varphi_t = |\Delta\varphi_{-3V}| + |\Delta\varphi_{+3V}|$, is represented in Table II at different frequencies. The phase shifts in Table II are promisingly large taking into account that the entire phase shifter has a length of only 1 mm.

The electromagnetic losses, represented in Fig. 3(b), decrease with increasing the bias. Thus, the losses at 1 GHz were -15.6 dB at a bias of -3 V and -6.3 dB at +3 V, and decrease with frequency up to $-4 - -5$ dB at 10 GHz, irrespective of the applied voltages. The losses are higher at lower frequencies because the thicknesses of the gold electrodes are only 200 nm, smaller that the skin depth, which is higher than 1 μm at 1 GHz. In future experiments we intend to use gold electroplating techniques to obtain more than 1 μm gold metallization over the entire structure, which would decrease the losses up to $-2 - -3$ dB.

Another source of losses at low frequencies, especially in the range 1-4 GHz, is the IDC configuration based on electromagnetic coupling, which can be represented by an equivalent series RC circuit, with C depending on the applied voltage. The resistance R decreases rapidly with frequency, attaining at 0 V values of 232 Ω at 1 GHz and of 126 Ω at 2.45 GHz. As such, the resistance of the equivalent circuit of the IDC configuration induces mismatch to the 50 Ω port impedance at low frequencies, and thus significant insertion loss, which becomes less evident as the frequency increases.

6

The capacitance of the structure, dependent on frequency f and the applied voltage V_{DC}, is computed as $C = -1/\omega \, \text{Im}[Z_{in}(f, V_{DC})]$, where $Z_{in}(f, V_{DC})$ is the input impedance of the coplanar structure, and it is represented in Fig. 4. This figure shows that the capacitance decreases with frequency and increases with the applied voltage, the increase being especially significant for V_{DC} between 2 and 3 V, where C increases about 4 times in the range 1-3 GHz. This behaviour explains the significant phase shift gained at low frequencies.

The nonlinear behaviour of phase and capacitance at lower frequencies (1-4 GHz) are due to nonlinear behaviour of the electrical permittivity of the ferroelectric with frequency a situation that can be observed in any ferroelectric in certain frequency range.

We have simulated the ferroelectric phase shifter using CST and compared with the experimental results. The results are displayed in Fig. 5. In Fig. 5a, we present the comparison between simulated (dashed lines) and measured (solid lines) scattering parameters (return loss – S11 – and transmission – S21), whereas Fig. 5b shows the simulated (dashed line) and measured (solid line) transmission phase, in the frequency range 1 – 11 GHz. The reference situation is with unbiased HfZrO, hence at 0 V. The overall behavior of the predicted (i.e. simulated) results is in rather good agreement with the measurements: the corresponding curves exhibit the same trend. The disagreements could be due to the limitations of the electromagnetic simulator, considering that the aspect ratio AR between the thin HfZrO layer and the bulk HRSi substrate is very high (if t_{HFZrO} and t_{HRSi} are the thickness of the HfZrO and HRSi layer, respectively, we have AR = t_{HRSi}/t_{HFZrO} = 87500); furthermore, the overall ferroelectric effect considered in the simulations was limited to the relative permittivity and dielectric losses, as extracted from the literature. This means that the ferroelectric's real characteristics can affect even significantly the agreement with the simulations.

We have measured the same devices annealed at 130°C for two hours. While the phase shift range for the -3 V to +3 V applied voltages remains almost the same, the capacitance

decreases with about 22%, preserving the same shape as in Fig. 4, which indicates that the ferroelectric effect becomes weaker.

4. Conclusions

In conclusion, we have demonstrated that a $Hf_{0.45}Zr_{0.55}O_{1.76}$ ferroelectric is able to produce a significant phase shift of electromagnetic signals in the range 1-10 GHz, at very low applied voltages. Further research will be dedicated to improve the losses of phase shifters and to integrate them in an antenna array in fully compatible CMOS technology.

8

References

[1] T.S. Böscke, J. Müller, D. Bräuhaus, U. Schröder, and U. Böttger, Ferroelectricity in hafnium oxide thin films, Appl. Phys. Lett. 99, 102903 (2011).

[2] J. Müller, T.S. Böscke, U. Schröder, S. Mueller, D. Bräuhaus, U. Böttger, L. Frey, and T. Mikolajick, Ferroelectricity in simple binary ZrO_2 and HfO_2, Nano Lett. 12, 4318−4323 (2012).

[3] U. Schröder, S. Mueller, J. Mueller, E. Yarchuk, D. Martin, C. Adelmann, T. Schloesser, R. van Bentum, and T. Mikolajick, Hafnium oxide based CMOS compatible ferroelectric materials, ECS J. Solid State Science and Technology 2, N69-N72 (2013).

[4] S. Starschich, T. Schenk, U. Schröder, and U. Böttger, Ferroelectric and piezoelectric properties of $Hf_{1-x}Zr_xO_2$ and pure ZrO_2 films, Appl. Phys. Lett. 110, 182905 (2017).

[5] S.W. Smith, A.R. Kitahara, M.A. Rodriguez, M.D. Henry, M.T. Brumbach, and J.I. Ihlefeld, Pyroelectric response in crystalline zirconium oxide ($Hf_{1-x}Zr_xO_2$) thin films, Appl. Phys. Lett. 110, 072901 (2017).

[6] F. Ambiz-Vargas, G. Kolhatkar, R. Thomas, R. Nouar, A. Sarkissian, C. Gomez-Yárez, M. Gauthier, and A. Ruediger, Tunneling electroresistance effect in a Pt/ $Hf_{0.5}Zr_{0.5}O_2$/Pt structure, App. Phys. Lett. 110, 093106 (2017).

[7] M. Dragoman, M. Aldrigo, M. Modreanu, and D. Dragoman, Extraordinary tunability of high frequency devices using $Hf_{0.3}Zr_{0.7}O_2$ ferroelectric at very low applied voltages, Appl. Phys. Lett. 110, 103104 (2017).

[8] A. Ahmed, I.A. Goldhorpe, and A.K. Khandani, Electrically tunable materials for microwave applications, Appl. Phys. Rev. 2, 011302 (2015).

[9] R.C. Hansen, *Phased Array Antennas*, 2nd edition, John Wiley and Sons, New York (2009).

[10] M. Modreanu, J. Sancho-Parramon, O. Durand, B. Servet, M. Stchakovsky, C. Eypert, C. Naudin, A. Knowles, F. Bridou, and M.-F. Ravet, Investigation of thermal annealing effects on microstructural and optical properties of HfO_2 thin films, Appl. Surf. Sci. 253, 328–334 (2006).

[11] A. Pal, V. K. Narasimhan, S. Weeks, K. Littau, D. Pramanik, and Tony Chiang, Enhancing ferroelectricity in dopant-free hafnium oxide, Appl. Phys. Lett. 110, 022903 (2017).

10

Table I. XPS High resolution Spectrum Quantification

Name	Position	% Conc.
O 1s	530.4	62.1
C 1s	284.7	2.6
Zr 3d	182.4	19.6
Hf 4d	17.1	15.7

Table II. Total phase $\Delta\varphi_t$/mm between -3 V and +3 V

Frequency (GHz)	$\Delta\varphi_{-3V}$	$\Delta\varphi_{+3V}$	$\Delta\varphi_t$
1	14.99^o	-51.24^o	66.23^o
2.45	18.92^o	-30.87^o	49.79^o
5.5	14.20^o	-14.56^o	28.76^o
10	8.78^o	-6.86^o	15.62^o

Figure captions

Fig. 1 (a) Scanning electron microscope (SEM) image of the phase shifter based on HfZrO.

Inset: optical microscope image; (b) GIXRD pattern for the HfZrO thin film on Si(100).

Fig. 2   Schematic representation of the measurement set-up.

Fig. 3   (a) The phase shift and (b) insertion loss as a function of applied bias and frequency.

Fig. 4   Capacitance of the equivalent circuit as a function of applied bias and frequency.

Fig. 5 Comparison between the simulated and measured results.
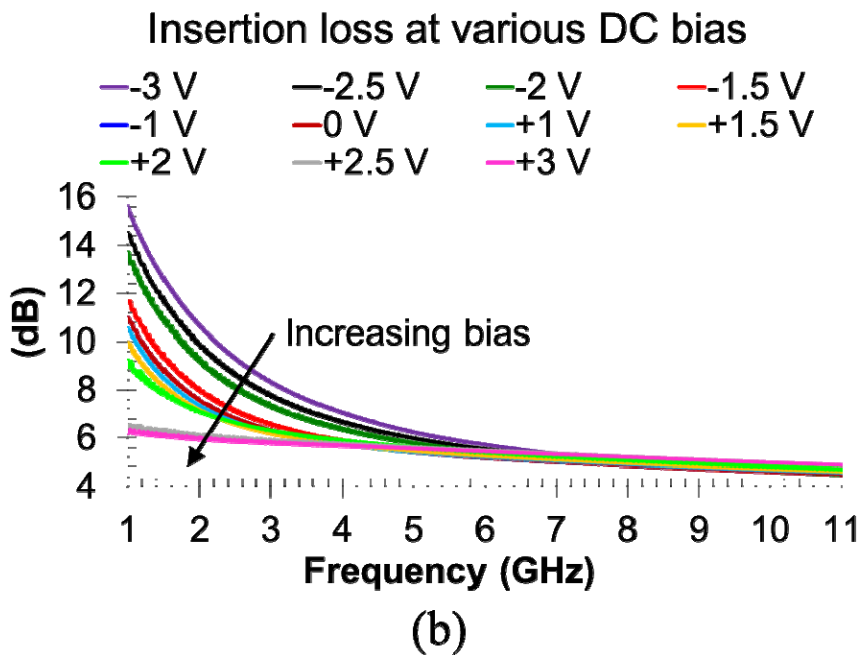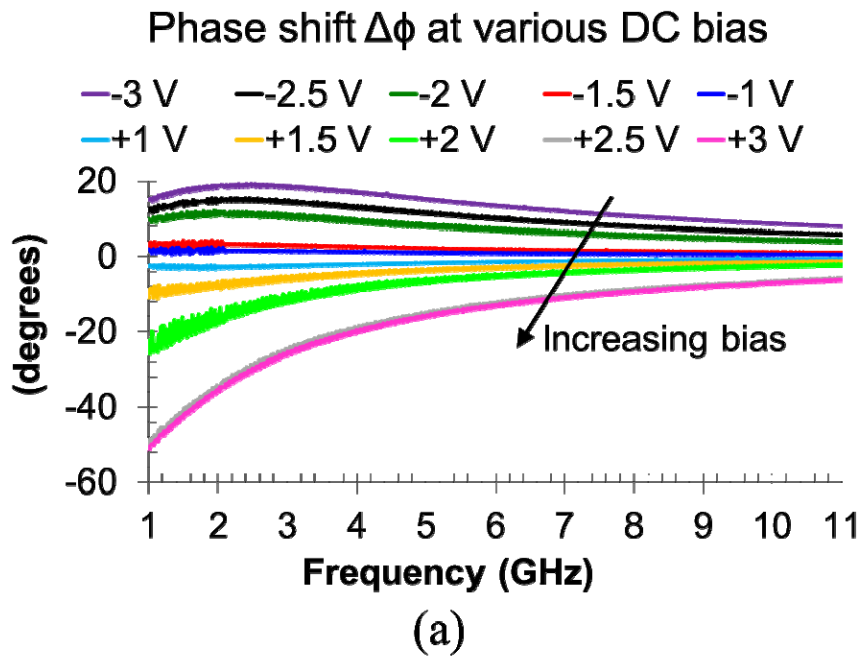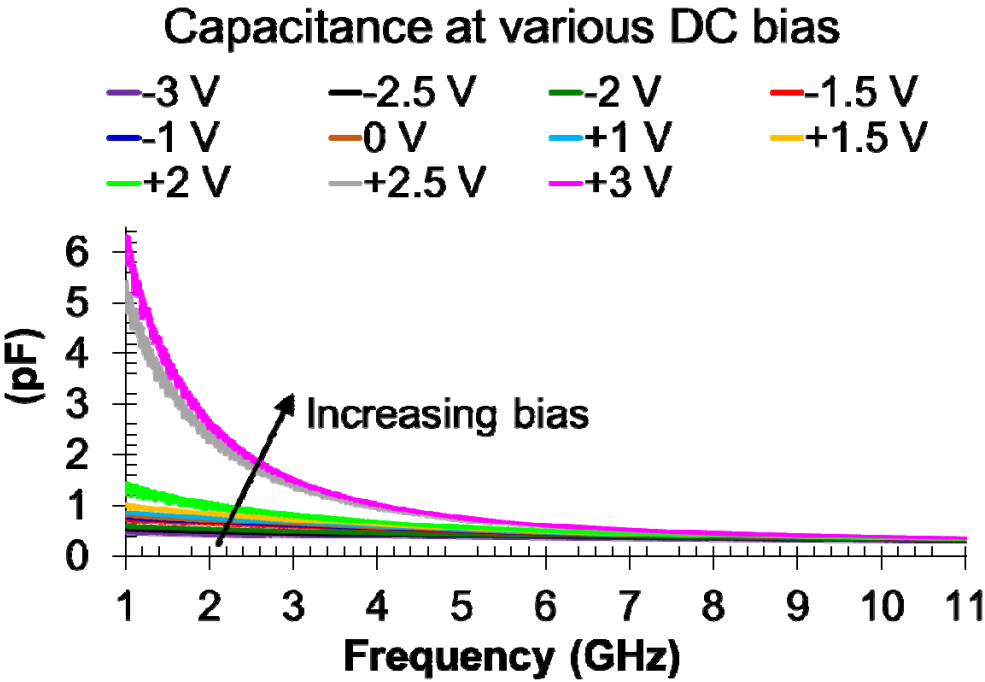
12

(a)

(b)

Fig. 1

13

1
2
3
4
5
6
7
8
9
10
11
12
13
14
15
16
17
18
19
20
21
22
23
24
25
26
27
28
29
30
31
32
33
34
35
36
37
38
39
40
41
42
43
44
45
46
47
48
49
50
51
52
53
54
55
56
57
58
59
60

Fig. 2

(a)

(b)

(a)

(b)

Fig. 3

15

Fig. 4

16

Fig. 5